A VARIATIONAL SHEARLET-BASED MODEL FOR AORTIC STENT DETECTION

Y. Farouj[1], L. Navarro[2], M. Clausel[3], P. Delachartre[1]

[1]University of Lyon; CREATIS; CNRS UMR 5220; Inserm U1044, Villeurbanne, France

[2]École Nationale Supérieure des Mines; CIS-EMSE; CNRS UMR 5307; LGF, F-42023 Saint-Etienne, France

[3] University of Grenoble-Alpes; Laboratoire Jean Kuntzmann; CNRS UMR 5224, Grenoble, France

ABSTRACT

In medical applications, stent segmentation in the abdominal aorta has to be carried out in challenging conditions, since one has to deal with noise, low contrast, objects having similar appearances and missing or blurred edges. Variational segmentation methods eases this task by carrying prior information on the target region or on the regularity of its boundaries. In this paper, we propose a new approach based on the global minimization of the Active Contour model using the L^1-norm of the Shearlet Transform instead of Total Variation (TV-norm). One of the distinctive features of such a regularization is that it allows the detection of anisotropic structures in images like stents boundaries. The sparsity imposed by the minimization provides piecewise smooth solutions with C^2-singularities. We also use the shearlet coefficients to construct an edge function for more faithful contour detection. Performances of our algorithm are evaluated on a stent segmentation from post-operative CT data. Results show that the proposed method drastically improves the detection of the stent placement compared to the TV based approach.

Index Terms— CT-imaging, Stent segmentation, Active contour, Shearlet Transform, Split Bregman algorithm

1. INTRODUCTION

The abdominal aortic aneurysm (AAA) is a common pathology consisting in a permanent dilatation of the abdominal aorta, which can reach a diameter twice higher than normal. A sudden rupture due to a weakening of the arterial wall may occur, which usually leads to the death of the patient. Two techniques exist for the treatment of AAA: the standard surgical procedure and the endovascular procedure. The first consists in incising the abdomen of the patient and replacing the weakened wall of the aneurysm by a woven polymer prosthesis (PTFE or PET). The second requires only two small incisions in the patient's groin, without opening the abdomen. Using a radiographic control device for the surgical procedure, a delivery sheath which contains the stent, is introduced through the femoral artery, from the groin up to the aorta. The stent is then deployed in the aneurysm. The system set up consists of a cylindrical surgical textile coating covering a cylindrical metallic mesh stent. The endoprosthesis becomes a blood driver which reduces blood pressure on the arterial wall, thereby stabilizing the aneurysm and preventing changes. Endovascular surgery carries less risk of perioperative complications than conventional surgery but several adverse events may occur in the longer term. Surgical re-interventions, often needed within five years after stenting, may come from poor positioning of the stent during the operation in tortuous or calcified vessels, or be due to poor sizing of the stent, which is done manually by surgeons from scanners examined in sizing software. Segmentation of stents in scanner images constitutes an important part of a project aiming at developing a finite element numerical simulation tool mimicking the release of a stent into custom geometries arteries. That allows the physician to choose the best stent and its dimensions for a specific patient, anticipating potential complications such as kinking, endoleak or malposition.

Segmentation is the process of dividing an image into different regions. This task is strongly related to the detection of curves enclosing these regions and has crucial applications in medical imaging such as in diagnosis, surgical planing and tumors progress analysis. Numerous techniques have been proposed to tackle the general segmentation problem along different models. Among these models, the variational ones have proven to be effective for medical images [1]. These last approaches were initiated by Mumford and Shah [2]. The idea is that an image can be approximated by a piecewise-smooth function. Smooth parts represent object while singularities are edges. Solving the problem related to this model means finding the best approximation of the image as well as its set of discontinuities. To overcome the numerical difficulties related to this last approach, Chan and Vese [3] proposed to minimize the Mumford-Shah energy for two regions (foreground and background) with a piecewise-constant assumption on the approximation function. Their idea was to represent the foreground region as the positive domain of a level-set function ϕ supposing that the boundary is bounded and closed. The characteristic functions of both regions are then obtained using the *Heaviside* step function of ϕ. The obtained energy is minimized with respect to ϕ driven by a gradient descent evolution. The drawback of this approach is the non-convexity of the underlying optimization problem

which makes the topology of the solution depending of the initial curves. We can assume that the initial curves are known only when the geometry of the segmented object is simple and known (for e.g. in the case where the object of interest are organs). A convex version which overcomes this difficulty was proposed by Chan and al.[4] inspired from the famous variational ROF model [5]. A global minimizer of the related energy can be obtained via a range of optimization techniques.

An other class of variational models is the geodesic active contour (GAC) [6]. It is based on the evolution of a closed boundary curve with a speed depending on an edge detecting function identifying relevant structures in the image. Various numerical schemes were proposed for this model, among them we can cite those based on Fast Marching techniques [7].

The approach we are presenting in this paper is related to the work of Bresson and al. in [8]. Their idea was to unify the convex Chan-Vese formulation and GAC techniques in a global active contour model. To this end, they introduce a weighted TV-norm regularization where the weight function is given by the edge detection function. The weight function aims to favor segmentation on the objects boundaries. In [9][10], the total variation was replaced by the L^1-norm of the wavelet transform of the image. This has two consequences of relevance to our problem. First wavelets coefficients contains more geometric information than the gradient at different scales, and second, the sparsity of wavelets coefficients imposes piecewise smoothness instead of the prohibitive piecewise constancy imposed by the sparsity of the TV-norm.

On the other hand, shearlets were introduced in [11] [12] as an efficient framework for the representation of multidimensional data. The shearlet representation have proven to overcome some of the limitations of traditional multiscale wavelet based representations as capturing anisotropic features. In opposition to the rotation-based directional selectivity used by curvelets, shearlets are based on shearing. This not only allows the construction of the shearlet system from a single generator, but also eases the derivation of faithful numerical aspect from the continuum theory as the shear operator preserve the integer lattice. The shearlet transform was already used in [13] as a regularizer for the segmentation of curved structures.

In this work, we use the shearlet framework to solve the global active contour model. This is done by using the L^1-norm of the shearlet coefficents as a regularization term. This is motivated by the fact that shearlets give sparse representation of smooth functions with C^2 singularities [11] like in a wide range of medical images [14]. Also, the shearlet transform provides good approximation of anisotropic features as contours. This fact encouraged us to construct a robust edge detection function to capture edges of different orders and scales. To solve the underlying optimization problem we will use the Split Bregman algorithm which have proven to be effective for minimization of L^1-regularized energies [15].

The rest of the paper is organized as follows. The shearlet transform is introduced in Section II. Section III contains a description of the proposed segmentation model along with the Split Bregman algorithm. In section IV, we show an application of our method from CT stent segmentation and we compare results to those obtained using a TV-norm.

2. SHEARLET TRANSFORM

We describe the continuous shearlet transform in $\mathbb{R}^2$. Let

$$A_a = \begin{bmatrix} a & 0 \\ 0 & \sqrt{a} \end{bmatrix}, a \in \mathbb{R}^+ \text{ and } S_s = \begin{bmatrix} 1 & s \\ 0 & 1 \end{bmatrix}, s \in \mathbb{R}$$

be respectively the parabolic (anisotropic) *scaling* matrix and the *shear* matrix acting on the plane. Let $\psi_{a,s,t} \in \mathbb{L}_2(\mathbb{R}^2)$ be the function derived from a function $\psi \in \mathbb{L}_2(\mathbb{R}^2)$ by dilatation, shearing and translation.

$$\psi_{a,s,t}(x) = a^{\frac{3}{4}} \psi\Big(A_a^{-1} S_s^{-1}(x-t)\Big), \tag{1}$$

where $t \in \mathbb{R}^2$ denotes the translation. Then, the *Fourier Transform* of $\psi_{a,s,t}$ is given by

$$\hat{\psi}_{a,s,t} = a^{\frac{3}{4}} \hat{\psi}\Big(a\omega_1, \sqrt{a}(s\omega_1 + \omega_2)\Big). \tag{2}$$

The shearlet system generated by ψ is defined by $\{\psi_{a,s,t} : a \in \mathbb{R}^+, s \in \mathbb{R}, t \in \mathbb{R}^2\}$. The associated continuous shearlet transform of a function $f \in \mathbb{L}_2(\mathbb{R}^2)$ is given by

$$\mathcal{SH}_\psi(f)(a,s,t) := \langle f, \psi_{a,s,t} \rangle = \langle \hat{f}, \hat{\psi}_{a,s,t} \rangle, \tag{3}$$

with $\hat{f}$ being the *Fourier Transform* of f. The shearlet ψ is called admissible if

$$\int_{\mathbb{R}^2} \frac{|\hat{\psi}(\omega_1, \omega_2)|^2}{|\omega|^2} \, \mathrm{d}\omega_1 \mathrm{d}\omega_2 < \infty.$$

The admissibility condition is important because it usually allows the reconstruction of the function f from the representation coefficients $\langle f, \psi_{a,s,t} \rangle$. Typical choices for shearlets are functions of the form :

$$\hat{\psi}(\omega) = \hat{\psi}_1(\omega_1)\hat{\psi}_2\Big(\frac{\omega_2}{\omega_1}\Big),$$

where $\psi_1 : \mathbb{R} \longrightarrow \mathbb{R}$ is a wavelet and ψ_2 is a bump function. For better directional selectivity, vertical and horizontal cones were introduced in [11]. The idea is to locally set the shearlets to zero in the *Fourier domain* by multiplying it by the characteristic functions of the cones. The first step consists in the discretization of the variables, therefore one builds discrete sets A, S for the scales a and shears s. Note that one usually choose a logarithmic scale for a and a linear scale

for s. The discret transforms we will use are based on cone-adapted shearlet systems with a translation invariance property. Notice that the discrete shearlets constitute a Parseval frame. This fact is crucial for the optimization algorithm we will be using. We refer to [16] for details on the implementation and the discretization of such transforms on a finite domain.

3. SEGMENTATION MODEL

Following a similar idea as the formulation of Mumford and Shah, The Active Contour Without Edges (ACWE) model of Chan and Vese aims to approximate an image $\mathbf{I} : \Omega \longrightarrow \mathbb{R}$ by a function taking two values characterizing two regions Ω_1 and $\Omega_2 = \Omega \backslash \Omega_1$. Let us note $Per(\Omega_1)$ the perimeter of their common boundary Γ. The energy to be minimized reads :

$$E_{CV}(\Omega, c_1, c_2) = \mu \int_{\Omega_1} (\mathbf{I}(x) - c_1)^2 \, \mathrm{d}x + \mu \int_{\Omega_2} (\mathbf{I}(x) - c_2)^2 \, \mathrm{d}x + Per(\Omega_1), \quad (4)$$

where Ω_1 is the segmented region, and c_i is the average intensity inside the region Ω_i for $i = \{1, 2\}$, while the parameter μ controls the strength of the data fidelity term. By taking Γ as the zero level set of a Lipschitz function $\phi : \Omega \longrightarrow \mathbb{R}$ and introducing a regularized *Heaviside* function H_ϵ, the minimization problem (4) yields to the associated Euler-Lagrange equation for ϕ

$$\partial_t \phi = H'_\epsilon(\phi)\Big(-\mu \, (\mathbf{I}(x) - c_1)^2 + \mu \, (\mathbf{I}(x) - c_2)^2 + \nabla . \frac{\nabla \phi}{|\nabla \phi|}\Big). \quad (5)$$

for fixed values of c_1 and c_2. The first two terms of the right hand side forces the contour to move in a direction that depends whether $\mathbf{I}(x)$ is closest to c_1 or c_2. The term with a divergence operator aims to impose smoothness on the contour. The optimization is then performed alternatively for ϕ and $(c_i)_{i=1,2}$. Note that, due to the $H'_\epsilon(\phi)$ factor, only local information is used to compute the level set evolution hence the optimization problem can not be globally convex. To overcome this fact, one can choose a smooth strictly monotone non-compactly supported approximation of the *Heaviside* function. Then the solution of (5) coincides with the state solution of

$$\partial_t \phi = -\mu \, (\mathbf{I}(x) - c_1)^2 + \mu \, (\mathbf{I}(x) - c_2)^2 + \nabla . \frac{\nabla \phi}{|\nabla \phi|}, \quad (6)$$

which is the Euler-Lagrange equation of the following energy :

$$|\nabla \phi|_1 + \mu \langle \phi, r \rangle \quad (7)$$

where $r(x, c_1, c_2) = (\mathbf{I}(x) - c_1)^2 - (\mathbf{I}(x) - c_2)^2$. This model has been combined with an edge based approach by replacing the standard TV norm by a weighted version depending on an positive edge indicator function $\mathcal{G}_\beta(x) = \dfrac{1}{1 + \beta ||\nabla \mathbf{I}(x)||^2}$ with $\beta \geq 0$, this favors segmentation along curves when $\mathcal{G}$ is minimal. Moreover a convex relaxation is usually made on ϕ over $[0, 1]$. A final thresholding step on the level set function gives the binary solution ($\Omega_1 = \{x \in \Omega \quad ; \quad \phi(x) > \sigma\}$) with $\sigma \in [0, 1]$. The minimization problem reads

$$\underset{0 \leq \phi \leq 1}{min} |\mathcal{G} . \nabla \phi|_1 + \mu \langle \phi, r \rangle \quad (8)$$

As we mentioned in the introduction, in our approach, we replace the TV-norm regularization by the L^1-norm of the shearlet transform. Our minimization problem is then

$$\underset{0 \leq \phi \leq 1}{min} |\mathcal{G}^{\mathcal{S}}_\beta . \mathcal{SH}_\psi(\phi)|_1 + \mu \langle \phi, r \rangle, \quad (9)$$

where the new edge indicator function is given by

$$\mathcal{G}^{\mathcal{S}}_\beta(x) = \frac{1}{1 + \beta ||\mathcal{SH}^1_\psi(\mathbf{I}(x))||^2},$$

where $\mathcal{SH}^1_\psi(\mathbf{I}(x))$ is a vector composed of shearlet coefficients at level 1. We believe that this particular formulation is useful to capture singularities of with C^2 orders at different scales independently of the contrast. Sparsity aims to detect edges but also helps to counter noise effects. To solve the minimization problem (9), we apply the Split Bregman method due to its simplicity and efficiency for solving L^1 regularized problems. This method consists in separating the L^1 and L^2 parts by introducing an auxiliary variable d. Then the problem reads

$$\underset{0 \leq \phi \leq 1, d}{min} |\mathcal{G}^{\mathcal{S}}_\beta . d|_1 + \mu \langle \phi, r \rangle + \frac{\lambda}{2} ||d - \mathcal{SH}_\psi(\phi)||^2, \quad (10)$$

where λ is the smoothing parameter. The problem is then solved alternatively for ϕ and d. The advantage of such a formulation is that for fixed d the problem is differentiable while it has a proximal gradient for fixed ϕ and so it can be solved using a weighted shrink operator [17] of the form

$$\textit{Shrink}_g(h, \alpha)(x) = max\{h(x) - \frac{\alpha}{g(x)}, 0\} \frac{h(x)}{|h(x)|}.$$

To force the equality constraint $d = \mathcal{SH}_\psi(\phi)$ an other auxiliary variable b is usually introduced. The resulting sequence of iterations is

$$(\phi^{k+1}, d^{k+1}) = \underset{0 \leq \phi \leq 1, d}{argmin} \; |\mathcal{G}^{\mathcal{S}}_\beta . d|_1 + \mu \langle \phi, r \rangle + \frac{\lambda}{2} ||d - \mathcal{SH}_\psi(\phi) - b^k||^2, \quad (11)$$

$$b^{k+1} = b^k + (\mathcal{SH}_\psi(\phi^k) - d^k). \quad (12)$$

As the shearlet transform constitutes a Parseval frame, the inverse transform coincides with the adjoint operator which leads to the algorithm in the next page.

Algorithm Split Bregman iterations for solving (9)

Require: $\lambda, \mu, \beta \in \mathbb{R}^+$ and $\sigma \in [0,1]$

while $||\phi^{k+1} - \phi^k|| < \delta$ **do**

$\bar{\phi}^{k+1} = \mathcal{SH}_\psi^T(d^k - b^k) - \frac{\mu}{\lambda} r(., c_1^k, c_2^k)$

$\phi^{k+1} = \max\{\min\{\bar{\phi}^{k+1}, 1\}, 0\}$

$d^{k+1} = \mathit{Shrink}_{1\setminus \mathcal{G}_\beta^s}(\mathcal{SH}_\psi(\phi^{k+1}) + b^k, \frac{1}{\lambda})$

$b^{k+1} = b^k + (\mathcal{SH}_\psi(\phi^{k+1}) - d^{k+1})$

$c_1^k = \int_{\Omega_1^k} \mathbf{I}(x)\, \mathrm{d}x$, and $c_2^k = \int_{\Omega_2^k} \mathbf{I}(x)\, \mathrm{d}x$

Find $\Omega_1^{k+1} = \{x \ : \phi^{k+1} > \sigma\}$

end while

4. EXPERIMENTAL RESULTS

In this section, We present an example to demonstrate the efficiency of our method by applying it to the detection of an endovascular stent (Fig.1) in a post-surgery CT image. Due to the appearance resemblance between the metallic stent material and the underlying tissue, the piecewise constancy assumption is clearly not appropriate and TV-norm based methods fail. The minimization problem (8) is also solved using the Split Bregman algorithm as in [18]. Notice, however, that for the TV case, differentiation yields to a Poisson equation which can be solved via the Gauss-Seidel (GS) iterative algorithm.

Fig. 1. An illustration showing the placement of an endovascular stent graft in an aortic aneurysm.

The image "rice" in Fig.2 is easy to segment by homogenizing the background. We use it here for a first experiment as we only aim at illustrating the improvement of using shearlets. We compare results obtained by a shearlet regularization to those obtained by TV-norm regularization when using the same set of parameters and choosing the same gradient based edge detection function.

In Fig.3, one can remark the good behaviour of our algorithm in segmenting anisotropic features. Moreover, objects stay separated which is not the case for the TV-norm (e.g in the outlined area).

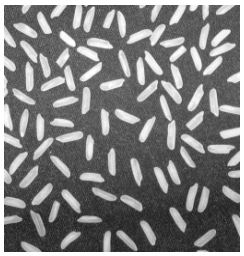

Fig. 2. Test image : rice

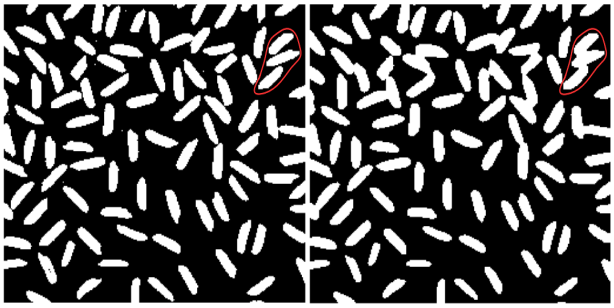

(a) (b)

Fig. 3. Ω_1 and Ω_2 obtained from the solution ϕ with $\sigma = 0.5$, $\mu = \lambda = 10^3$. (a) : Shearlet, (b) : TV.

Fig.4 and Fig.5 show an example of stent segmentation after tuning the parameters (μ, λ). Algorithms for both methods converge in 5 iterations while the average number of inner GS iterations required in the TV case is 9.8.

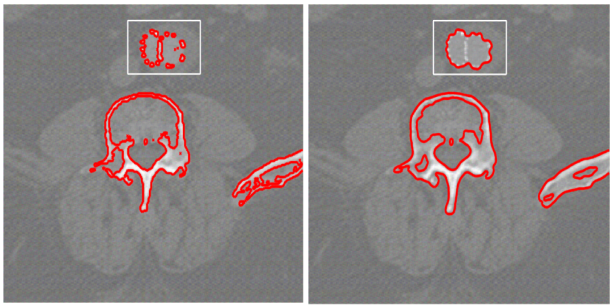

(a) (b)

Fig. 4. Contours from the segmentation of a CT image of the abdominal aorta (stent area outlined). $\sigma = 0.5$, $\mu = 10^4$, $\lambda = 0.5 \times \mu$. (a) : Shearlet, (b) : TV.

The boundaries of a cross section from the 3-dimensional cylindrical metallic mesh are efficiently detected by the shearlet based method. Notice that some of the pixels that are representing the inside of the abdominal aorta have values which are more close to those of pixels representing the stent than the rest of the image. These values are actually calcifications

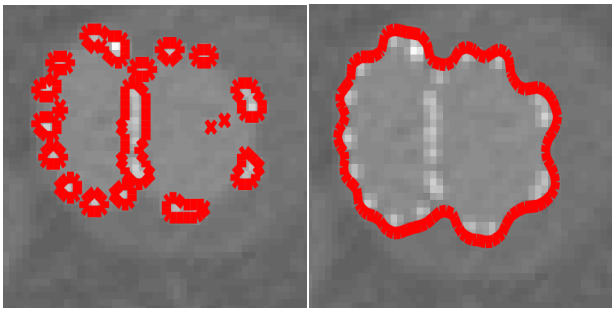

(a) (b)

Fig. 5. Zoom on the stent region. (a) : Shearlet, (b) : TV.

of the aorta and constitute an important difficulty in stent segmentation. TV-norm based methods are sensitive to this type of distributions as the regularization imposes piecewise constancy and so the results are not satisfying.

5. CONCLUSION

We proposed a new approach for the detection and visualization of stent structures in the abdominal aorta. Our method is relying on a new regularization motivated by some nice properties of the shearlet transform. We tested the algorithm on real images and showed that our new regularization provides a good approximation of the stent placement. For an ideal visualization, $3D$ segmentation is more appropriate. For this purpose, a model including 3-dimensional shearlets will be the subject of a future work.

Acknowledgements

This work was supported by "Région Rhône-Alpes" under the ARC 6. The authors would like to thank the Vascular Surgery Service of The Saint-Etienne CHU for the stent images. M. Clausel's research was supported by the French Agence Nationale de la Recherche (ANR) under reference ANR-13-BS03-0002-01 (ASTRES). P. Delachartre is within the framework of the Labex CELYA ANR-10-LABX-0060 of Université de Lyon.

6. REFERENCES

[1] R. Malladi, R. Kimmel, D. Adalsteinsson, G. Sapiro, V. Caselles, and J. A. Sethian, "A geometric approach to segmentation and analysis of 3d medical images," in *Proc. 1996 Workshop on Mathematical Methods in Biomedical Image Analysis (MMBIA'96), Washington, DC*, 2003, p. 1224.

[2] D. Mumford and D. Shah, "Optimal approximation by piecewise smooth functions and associated variational problems," *Commun. Pure Appl. Math*, vol. 42, pp. 577–685, 1989.

[3] T. F. Chan and L. A. Vese, "Active contours without edges," *IEEE Trans. Image Processing*, vol. 10, pp. 266–277, 2001.

[4] T. F. Chan, S. Esedoglu, and M. Nikolova, "Algorithms for finding global minimizers of image segmentation and denoising models," *SIAM J. Appl. Math*, vol. 66, pp. 1932–1648, 2006.

[5] L. Rudin, S. Osher, and E. Fatemi, "Nonlinear total variation based noise removal algorithms," *Physica D*, vol. 60, pp. 259–268, 1992.

[6] M. Kass, A. Witkin, and D. Terzopoulos, "Snakes: Active contour models," *International Journal of Computer Vision*, pp. 321–331, 1987.

[7] J. A. Sethian, "Level set methods and fast marching methods," *Interfaces in Comptational Geometry, Fluid Mechanics, Computer Vision and Materials Science. Cambridge University Press, Cambridge*, 1999.

[8] X. Bresson, S. Esedoglu, P. Vandergheynst, J. Thiran, and S. Osher, "Fast global minimization of the active contour/snake model," *J. Math. Imaging Vis.*, vol. 28, no. 2, pp. 151–167, 2007.

[9] C. Tai, X. Zhang, and Z. Shen, "Wavelet frame based multiphase image segmentation," *SIAM J. Imaging sci*, vol. 6, no. 4, pp. 2521–2546, 2013.

[10] B. Dong, A. Chien, and Z. Shen, "Frame based segmentation for medical images," *Communications in Mathematical Sciences*, vol. 9, no. 2, pp. 551–559, 2011.

[11] K. Guo, G. Kutyniok, and D. Labate, "Sparse multidimensional representations using anisotropic dilatation and shear operators," *Mod. Methods Math, Nashboro Press, Brentwood, TN*, pp. 189–201, 2006.

[12] D. Labate, W.-Q. Lim, G. Kutyniok, and G. Weiss, "Sparse multidimensional representations using shearlets," *Wavelets XI, SPIE Proc, 5914, Bellingham, WA*, 2005.

[13] S. Häuser and G. Steidl, "Convex multiclass segmentation with shearlet regularization," *International Journal of Computer Mathematics*, vol. 90, no. 1, pp. 62–81, 2013.

[14] E. J. Candès and D. L. Donoho, "New tight frames of curvelets and optimal representations of objects with piecewise c singularities," *Comm. Pure and Appl. Math*, pp. 219–266, 2002.

[15] T. Goldstein and S. Osher, "The split bregman method for l1-regularized problems.," *SIAM J. Imaging Sciences*, vol. 2, no. 2, pp. 323–343, 2009.

[16] S. Häuser, "Fast finite shearlet transform: a tutorial," *Preprint University of Kaiserslautern*, Preprint.

[17] I. Daubechies, M. Defrise, and C. De Mol, "An iterative thresholding algorithm for linear inverse problems with a sparsity constraint," *Comm. on Pure and Applied Mathematics*, , no. 11, pp. 1413–1457.

[18] Tom Goldstein, Xavier Bresson, and Stanley Osher, "Geometric applications of the split bregman method: Segmentation and surface reconstruction," *J. Sci. Comput.*, vol. 45, no. 1-3, pp. 272–293, Oct. 2010.